

Peripapillary Versus Macular Combined Hamartoma of the Retina and Retinal Pigment Epithelium: Imaging Characteristics



RAJAN GUPTA, ADRIAN T. FUNG, MARCO LUPIDI, RAJEEV R. PAPPURU, SAMEERA NAYAK, NIROJ KUMAR SAHOO, SWATHI KALIKI, LAWRENCE YANNUZZI, KATE REID, LIANNE LIM, RICCARDO SACCONI, VIVEK DAVE, SUMIT RANDHIR SINGH, APOORVA AYACHIT, PIERRE-HENRY GABRIELLE, SOPHIE CAI, LUIZ H. LIMA, GIUSEPPE QUERQUES, J. FERNANDO AREVALO, K. BAILEY FREUND, CAROL L. SHIELDS, AND JAY CHHABLANI

- **PURPOSE:** To compare clinical, optical coherence tomography (OCT), and fundus autofluorescence (FAF) characteristics of peripapillary vs macular variants of combined hamartoma of the retina and retinal pigment epithelium (combined hamartoma).
- **DESIGN:** Retrospective observational, comparative case series.
- **METHODS:** **SETTING:** Multicenter collaborative study. **STUDY POPULATION:** Fifty eyes with a clinical diagnosis of combined hamartoma. **OBSERVATIONAL ANALYSIS:** A comparative analysis of color fundus photographs (CFPs), OCT, and FAF was performed for peripapillary and macular variants of combined hamartoma. **MAIN OUTCOME MEASURES:** Pigmentation and OCT features of macular and peripapillary combined hamartoma.

AJO.com

Supplemental Material available at AJO.com.

Accepted for publication Jan 18, 2019.

From the Smt. Kanuri Santhamma Centre for Vitreo-Retinal Diseases (R.G., R.R.P., S.N., N.K.S., V.D., S.R.S., J.C.) and The Operation Eyesight Universal Institute for Eye Cancer (S.K.), L V Prasad Eye Institute, Hyderabad, India; Westmead Hospital, Sydney, New South Wales, Australia (A.T.F.); Faculty of Medicine and Health Sciences, Macquarie University, Sydney, New South Wales, Australia (A.T.F.); Save Sight Institute, University of Sydney, Sydney, New South Wales, Australia (A.T.F.); Department of Biomedical and Surgical Sciences, Section of Ophthalmology, University of Perugia, S. Maria della Misericordia Hospital, Perugia, Italy (M.L.); LuEsther T. Mertz Retinal Research Center, Manhattan Eye, Ear, and Throat Hospital, New York, New York, USA (L.Y., K.B.F.); Department of Ophthalmology, New York University, New York, New York, USA (L.Y., K.B.F.); Vitreous Retina Macula Consultants of New York, New York, New York, USA (L.Y., K.B.F.); Department of Ophthalmology, Canberra Hospital, Canberra, Australian Capital Territory, Australia (K.R.); School of Clinical Medicine, Australian National University, Canberra, Australian Capital Territory, Australia (K.R.); Ocular Oncology Service, Wills Eye Hospital, Philadelphia, Pennsylvania, USA (L.L., C.L.S.); Department of Ophthalmology, University Vita-Salute, IRCCS Ospedale San Raffaele, Milan, Italy (R.S., G.Q.); Department of Vitreoretina, M M Joshi Eye Institute, Hubballi, Karnataka, India (A.A.); Ophthalmology Department, Dijon University Hospital, Dijon, France (P.H.G.); Center for Taste and Feeding Behaviour, INRA, UMR1324, Dijon, France (P.H.G.); Retina Division, Wilmer Eye Institute, Johns Hopkins University School of Medicine, Baltimore, Maryland, USA (S.C., J.F.A.); and Federal University of São Paulo, São Paulo, Brazil (L.H.L.).

Inquiries to Jay Chhablani, Smt. Kanuri Santhamma Centre for Vitreo-Retinal Diseases, L V Prasad Eye Institute, Banjara Hills, Hyderabad 34, India; e-mail: jay.chhablani@gmail.com

- **RESULTS:** The review of imaging from 50 eyes of 49 patients diagnosed with combined hamartoma identified 18 (36%) peripapillary lesions, 27 (54%) macular lesions, and 5 (10%) peripheral lesions. A comparative analysis of peripapillary vs macular combined hamartoma identified differences in the following features: lesion pigmentation on CFPs corresponding to hypoautofluorescent FAF (88% vs 0%, $P < .001$) and OCT features of full-thickness involvement (88% vs 3%, $P < .001$), preretinal fibrosis (27% vs 81%, $P < .001$), maxi peaks (5% vs 88%, $P < .001$), intraretinal cystoid spaces (72% vs 40%, $P < .038$), outer plexiform layer involvement (5% vs 96%, $P < .001$), ellipsoid zone disruption (83% vs 3%, $P < .001$), RPE disruption (77% vs 3%, $P < .001$), and choroidal neovascularization (16% vs 0%, $P = .028$).
- **CONCLUSIONS:** This comparative analysis identified a higher frequency of pigmentation with hypoautofluorescence, full-thickness retinal involvement, intraretinal cystoid spaces, ellipsoid zone disruption, RPE disruption, and choroidal neovascularization in peripapillary combined hamartoma. These findings suggest that lesions occurring near or at the optic nerve are associated with a more severe degree of pigmentary changes and retinal disruption than those located in the macula. (*Am J Ophthalmol* 2019;200:263–269. © 2019 Elsevier Inc. All rights reserved.)

THE TERM “COMBINED HAMARTOMA OF RETINA AND retinal pigment epithelium” (combined hamartoma) was first coined by Gass¹ to describe a pigmented, elevated, charcoal gray hamartomatous malformation involving retinal pigment epithelium (RPE), retina, overlying retinal vasculature, and vitreoretinal interface. Based on the location and the common clinical characteristics, Gass classified combined hamartoma into 4 anatomically based groups: papillary, peripapillary, macular, or peripheral.

In 1969, Vogel and associates² published on the histopathology of peripapillary combined hamartoma, describing total retinal disorganization and a peculiar filigree pattern of pigmentation extending anteriorly into the retina and optic nerve head, and this formed the basis of the

TABLE. Comparison of Optical Coherence Tomography and Autofluorescence Features of Peripapillary vs Macular “Combined Hamartoma of the Retina and Retinal Pigment Epithelium” Lesions

Imaging Features	Peripapillary CHRRPE N = 18	Macular CHRRPE N = 27	P Value
OCT features			
Retinal involvement			
Full thickness	88% (16/18)	3% (1/27)	<.001
Partial thickness	11% (2/18)	96% (26/27)	<.001
Retinal features			
Preretinal fibrosis	27% (5/18)	81% (22/27)	<.001
Mini peaks	61% (11/18)	44% (12/27)	.273
Maxi peaks	5% (1/18)	88% (24/27)	<.001
OPL involvement (sawtooth/omega sign)	5% (1/18)	96% (26/27)	<.001
Intraretinal cystoid spaces	72% (13/18)	40% (11/27)	.038
Ellipsoid zone disruption (focal/diffuse)	83% (15/18)	3% (1/27)	<.001
Subretinal lipofuscin	11% (2/18)	None	.075
RPE disruption (irregularity/hypertrophy)	77% (14/18)	3% (1/27)	<.001
Choroidal neovascularization	16% (3/18)	None	.028
Autofluorescence			
Hypoautofluorescence	88% (16/18)	None	<.001

CHRRPE = combined hamartoma of the retina and retinal pigment epithelium; OCT = optical coherence tomography; OPL = outer plexiform layer; RPE = retinal pigment epithelium.

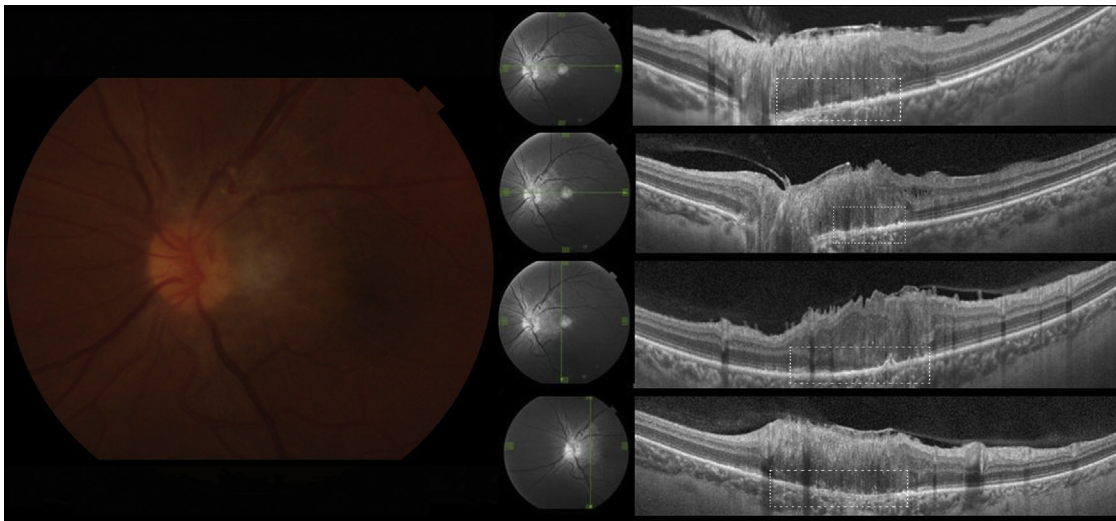


FIGURE 1. A multipanel collage image of a peripapillary combined hamartoma of retina and retinal pigment epithelium lesion in a 31-year-old woman with visual acuity of 20/100 in left eye showing characteristic mottled or mossy pattern of pigmentation on color fundus photograph. Swept-source optical coherence tomography cuts passing through multiple sites depict marked disorganization of retina along with disruption of ellipsoid zone and retinal pigment epithelium irregularities (dotted rectangle).

description of combined hamartoma given by Gass. However, owing to the morphologic resemblance of peripapillary and macular variants, the diagnosis of combined hamartoma was used for both.

More recently, optical coherence tomography (OCT) has revealed novel findings in the retinal microanatomy in cases of combined hamartoma, including prominent epiretinal membrane,³ minor vertical vitreoretinal trac-

tion (mini peaks),⁴ major vertical vitreoretinal traction with retinal folding of inner retinal layers (maxi peaks),^{4,5} and distortion of the outer plexiform layer (OPL)⁶ (sawtooth configuration or omega sign). However, most of these findings have been reported in macular lesions. There has been no study to date to compare the OCT features of combined hamartoma at different sites in the fundus.

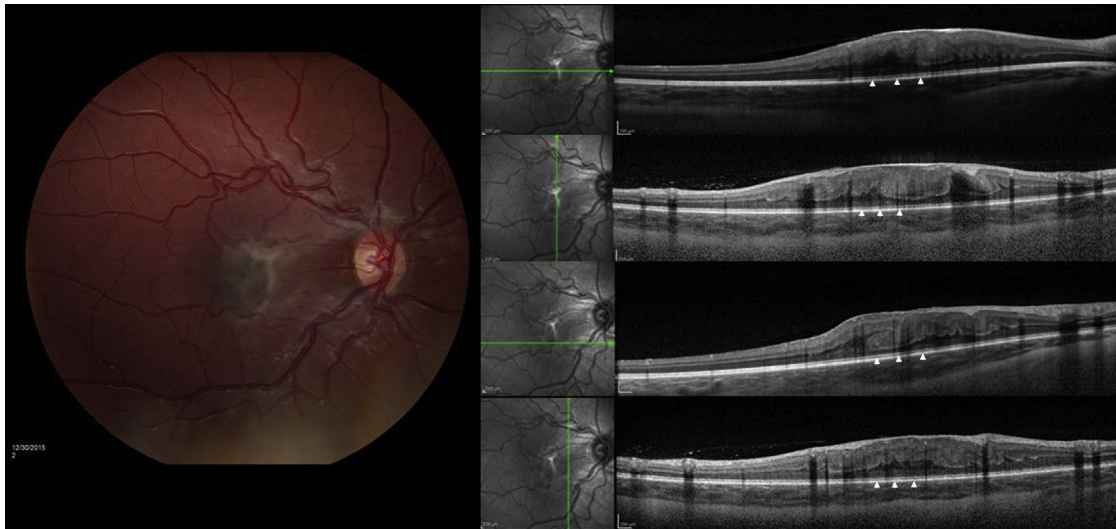


FIGURE 2. A multipanel collage image of a macular combined hamartoma of retina and retinal pigment epithelium (RPE) lesion in a 5-year-old girl with visual acuity of 20/400 in right eye showing attenuated subretinal pigmentation (grayish hue), prominent epiretinal membrane, and glial tissue on color fundus photograph. Spectral-domain optical coherence tomography cuts through multiple sites showing inner retinal disorganization (maxi peaks) limited by outer plexiform layer (omega sign) with relatively preserved outer retinal layers and intact RPE in all the sections (arrowheads).

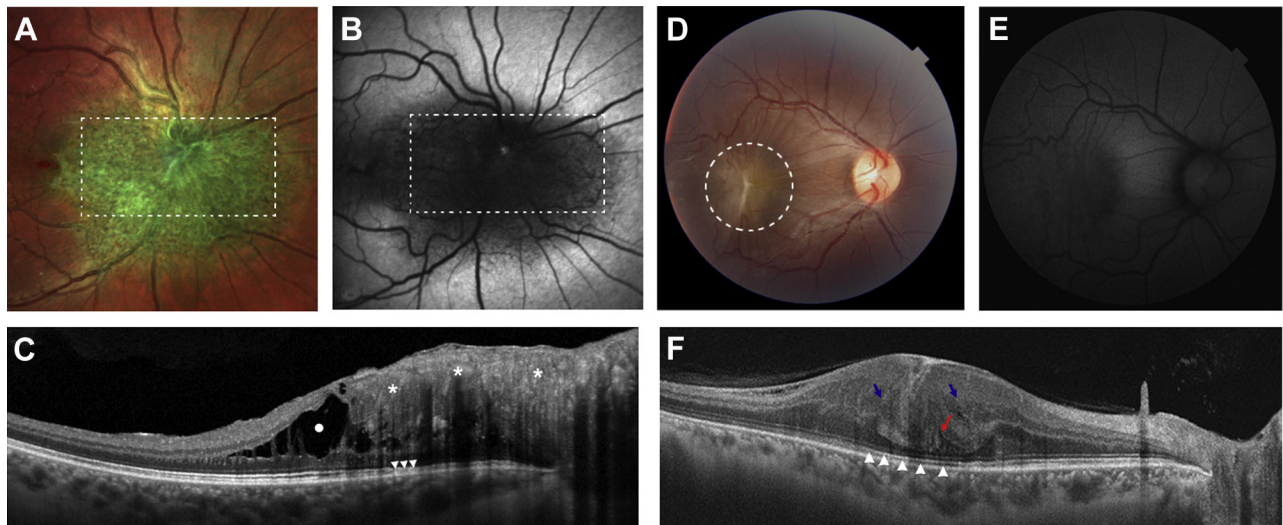


FIGURE 3. (A–C) Peripapillary combined hamartoma of retina and retinal pigment epithelium (combined hamartoma) lesion in a 35-year-old woman with visual acuity of 20/20 in right eye showing prominent epiretinal pigment migration on multicolor fundus photograph (A; dotted rectangle) with corresponding hypoautofluorescence obscuring superficial retinal vasculature on autofluorescence (B; dotted rectangle). Spectral-domain optical coherence tomography passing through the lesion (C) depicts marked disorganization of retina without any discernible inner retinal layers (asterisk), degenerative cystic changes (solid dot), and disruption of ellipsoid zone (arrowheads). (D–F) Macular combined hamartoma lesion in a 20-year-old man with a visual acuity of 20/40 in right eye showing attenuated subretinal pigmentation (D; dotted circle) not replicating on autofluorescence (E) and prominent preretinal fibrosis; corresponding swept-source optical coherence tomography (F) showing inner retinal disorganization (maxi peaks; blue arrows) limited by outer plexiform layer (omega sign; red arrow) with relatively preserved outer retinal layers (arrowheads).

Herein, we sought to compare the clinical, OCT, and fundus autofluorescence (FAF) characteristics of peripapillary and macular combined hamartoma, with an objec-

tive of providing a synoptic understanding of combined hamartoma in relation to the anatomic location of the lesion.

METHODS

THIS WAS A MULTICENTER COLLABORATIVE RETROSPECTIVE analysis of medical records and retinal imaging from 50 eyes of 49 patients diagnosed with combined hamartoma at 9 tertiary vitreoretinal practices from Australia, Italy, India, and the United States of America from January 2011 to April 2018. The local institutional review boards at each study site approved the study and the procedures adhered to the tenets of the Declaration of Helsinki. Written informed consent was obtained from all the participants at the time of enrollment.

• **PATIENT ELIGIBILITY:** Patients with a clinical diagnosis of combined hamartoma who underwent imaging with color fundus photography (Zeiss FF 450, Germany; Topcon TRC 50IX fundus camera, Topcon Medical Systems, Inc, Tokyo, Japan; RetCam, Massie Laboratories, Dublin, California, USA); OCT imaging with either swept-source OCT (SSOCT; DRI OCT Triton; Topcon Medical Systems, Inc, Tokyo, Japan), spectral-domain OCT (SDOCT; Heidelberg Spectralis HRA; Heidelberg Engineering, Heidelberg, Germany), or Cirrus SDOCT (Carl Zeiss Meditec, Dublin, California, USA); and FAF (Heidelberg Spectralis, Heidelberg Engineering, Heidelberg, Germany; Topcon TRC 50IX fundus camera, Topcon Medical Systems, Inc, Tokyo, Japan; DRI OCT Triton, Topcon Medical Systems, Inc, Tokyo, Japan) were included. The clinical diagnosis of combined hamartoma was made on the basis of clinical characteristics as described by Gass.¹

Cases with any other coexisting retinal disease contributing to epiretinal membrane (ERM), subretinal scarring, extensive fibrosis, or prominent back-shadowing on OCT obscuring the outer retinal details and cases with inconclusive diagnosis were excluded. Eyes with time-domain (TD) OCT or SDOCT scans without enhanced depth imaging (EDI) and low-resolution images were also excluded from the study.

• **PATIENT EVALUATION:** The data collection included information on patient demographics, ophthalmic features, clinical features, and imaging findings of combined hamartoma. Patient demographics included age and sex of the patients. Ophthalmic findings included best-corrected visual acuity (BCVA) in Snellen fraction converted into logarithm of the minimal angle of resolution (logMAR) for statistical analysis, anterior segment findings by slit-lamp evaluation, and intraocular pressure by applanation tonometry (mm Hg).

• **CLINICAL EVALUATION: Topography.** Based on color fundus photography, lesions were classified into the following:

- Papillary/Peripapillary: Lesions involving retina to within 1 mm from the optic disc as center.

- Macular: Lesions involving macula spanning up to 1-disc diameter-radius circle with foveola as center.
- Peripheral: Any lesion located outside the superior or inferior retinal vascular arcades or beyond the extent defined for macular or peripapillary lesions temporally and nasally.

Pigmentation. Pigmentation was defined as fine, mottled, mossy, or filigree pattern of pigmentary changes observed in the color fundus photographs that were considered significant only when corroborated with the hypoautofluorescence pattern obscuring the superficial retinal vasculature on autofluorescence.

• **OPTICAL COHERENCE TOMOGRAPHY ANALYSIS:** All patients underwent imaging on SSOCT or EDI SDOCT. Raster scans centered over each combined hamartoma were analyzed. The quantitative evaluation of OCT images included central macular thickness (CMT) measurements using the built-in caliper tool. Qualitative assessment included defining the extent of involvement by combined hamartoma based on the following:

- (1) Thickness
 - Full thickness: Grossly disorganized retinal morphology along with involvement of all retinal layers including OPL, ellipsoid zone (EZ), and RPE.
 - Partial thickness: Partially disorganized retinal architecture with involvement restricted to the inner retinal layers, limited by OPL.
- (2) Vitreoretinal interface anomalies: Preretinal fibrosis and mini peaks
- (3) Vitreoretinal interface anomalies: Infolding of inner retinal layers—maxi peaks
- (4) Distortion of OPL: Sawtooth appearance or omega sign
- (5) EZ disruption: Focal or diffuse
- (6) RPE involvement: hypertrophy, irregularity, or elevations.
- (7) Presence or absence of intraretinal cystoid changes.

All images were exported and shared with the principal investigator (J.C.). All images were analyzed by 2 observers (J.C. and R.G.), and mutual consensus was considered before making a final decision. Statistical significance (P value < .05) of the above-mentioned variables on OCT and FAF were calculated using χ^2 test.

RESULTS

IMAGING FROM 50 EYES OF 49 PATIENTS WITH A CLINICAL diagnosis of combined hamartoma and meeting inclusion

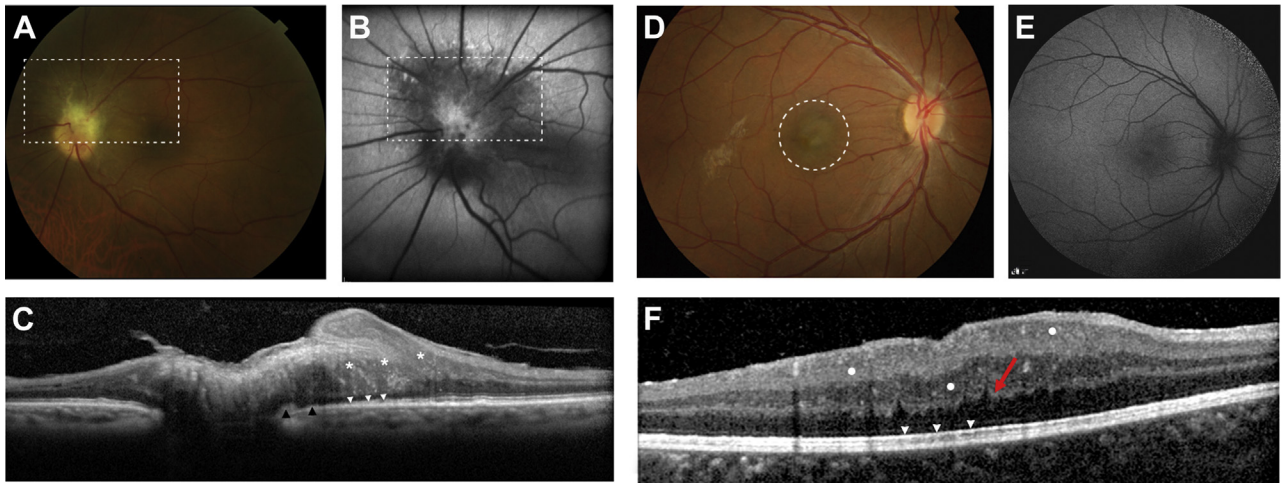


FIGURE 4. (A–C) Peripapillary combined hamartoma of retina and retinal pigment epithelium (combined hamartoma) lesion in a 72-year-old man with visual acuity of 20/80 in left eye showing characteristic mottled or mossy pattern of pigmentation on color fundus photograph (A; dotted rectangle) with corresponding hypoautofluorescence obscuring superficial retinal vasculature on autofluorescence (B; dotted rectangle). Spectral-domain optical coherence tomography passing through the lesion (C) depicts marked disorganization of retina (asterisks) along with disruption of ellipsoid zone (white arrowheads) and retinal pigment epithelium irregularity (black arrowheads). (D–F) Macular combined hamartoma lesion in a 10-year-old male subject with a visual acuity of 20/400 in left eye showing attenuated subretinal pigmentation (D; dotted circle) not discernible on autofluorescence (E) and corresponding spectral-domain optical coherence tomography (F) showing disorganized but still discernible inner retinal layers (solid dots) limited by outer plexiform layer (sawtooth appearance; red arrow) with relatively preserved outer retinal layers (arrowheads).

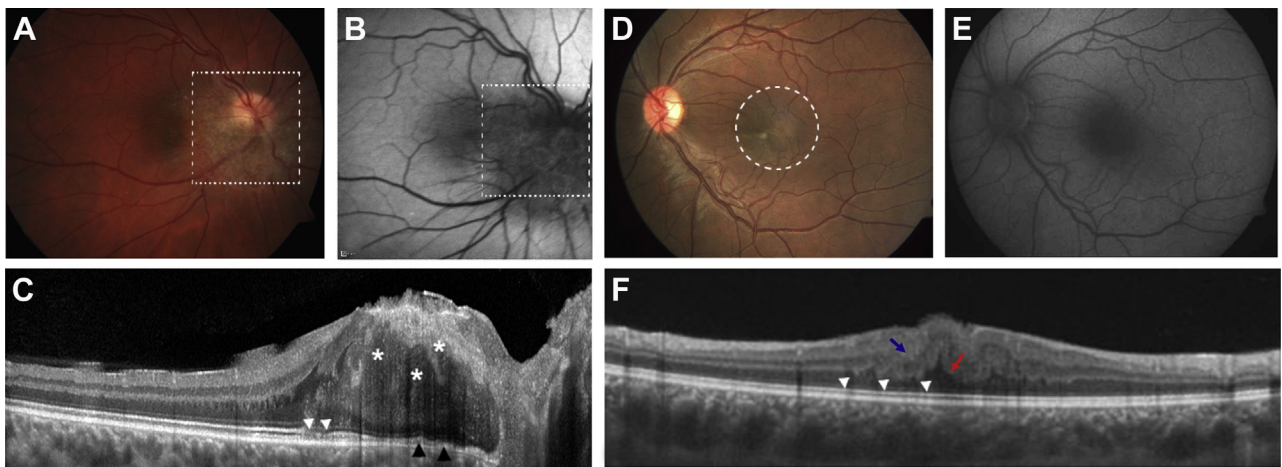


FIGURE 5. (A–C) Peripapillary combined hamartoma of retina and retinal pigment epithelium (combined hamartoma) lesion in a 28-year-old man with visual acuity of 20/50 in right eye showing prominent peripapillary pigmentation on color fundus photograph (A; dotted rectangle) with corresponding hypoautofluorescence obscuring superficial retinal vasculature on autofluorescence (B; dotted rectangle). Spectral-domain optical coherence tomography passing through the lesion (C) depicts marked disorganization of retina without any discernible inner retinal layers (asterisks) along with focal disruption of ellipsoid zone (white arrowheads) and retinal pigment epithelium irregularity (black arrowheads). (D–F) Macular combined hamartoma lesion in a 17-year-old male subject with visual acuity of 20/125 in the left eye showing attenuated subretinal grayish hue (D; dotted circle) not replicating on autofluorescence (E), preretinal fibrosis, and the corresponding swept-source optical coherence tomography (F) showing inner retinal disorganization (maxi peaks; blue arrow) limited by outer plexiform layer (sawtooth appearance; red arrow) and relatively preserved outer retinal layers (arrowheads).

criteria was analyzed. The mean patient age at the time of image acquisition was 23 ± 18 years, with 28 male and 21 female patients. All but 1 lesion occurred unilaterally. Mean age for the patients with peripapillary lesions with pigmentation was higher (27 years) as compared to the macular lesions with preretinal fibrosis (14.5 years).

Out of 50 eyes, 18 (36%) were peripapillary, 27 (54%) were macular, and 5 (10%) were peripheral in location. Overall mean (\pm standard deviation) BCVA was 0.94 ± 0.97 logMAR (Snellen equivalent: 20/160). A comparative analysis based on the location (peripapillary vs macular) of combined hamartoma revealed significant differences in mean BCVA (0.50 ± 0.42 logMAR vs 1.34 ± 1.18 logMAR, $P = .0011$) (Snellen equivalent: 20/70 vs 20/400) and mean CMT ($392.3 \pm 99.9 \mu\text{m}$ vs $586.9 \pm 111.3 \mu\text{m}$, $P < .001$). The mean CMT irrespective of location of combined hamartoma was $486 \pm 152.7 \mu\text{m}$.

A filigree pattern of pigmentation on color fundus photographs corresponding to a hypoautofluorescent pattern of FAF was only evident in peripapillary variants (88% vs 0%, $P < .001$). There was no obvious pigmentation in the macular variant but there was a subtle subretinal grayish hue, which did not correlate with FAF features.

Comparative analysis of OCT features of peripapillary vs macular combined hamartoma (Table) revealed significant differences in full-thickness retinal involvement (88% vs 3%, $P < .001$), preretinal fibrosis (27% vs 81%, $P < .001$), maxi peaks (5% vs 88%, $P < .001$), intraretinal cystoid spaces (72% vs 40%, $P < .038$), OPL involvement (5% vs 96%, $P < .001$), EZ disruption (83% vs 3%, $P < .001$), RPE disruption (77% vs 3%, $P < .001$), and choroidal neovascularization (16% vs 0%, $P = .028$), which were statistically significant. Nonsignificant differences were observed in other OCT features, including mini peaks (61% vs 44%) and subretinal lipofuscin (11% vs 0%). Presence of ectopic inner foveal layers, which have been recently described in the context of grade 4 epiretinal membranes, was a noteworthy association, seen in 26 out of 27 macular cases evaluated.

DISCUSSION

THE DISCREPANCY AND VARIATION IN THE CLINICAL PRESENTATION of macular and peripapillary combined hamartoma has been contested by Gass in his case series of 7 patients, which led to the inception of combined hamartoma. Variability in pigmentation, which was more evident and widespread in cases of peripapillary lesions as compared to the macular variants, was reported. The filigree pattern of pigmentation seen in peripapillary combined hamartoma correlated with the histopathologic evidence stating marked proliferation of juxtapapillary pigment epithelium into the overlying retina and the optic nerve head. The reduplication of monolayered RPE beneath the lesion, seen in the histologic sections of peripapillary combined hamartoma, was

thought to be a cause of subtle and attenuated pigmentation seen in cases of macular hamartoma lesions.

The hypoautofluorescence pattern obscuring the superficial retinal vasculature seen in the peripapillary cases adheres to the clinical description and the pathophysiological basis for the description of combined hamartoma in the literature. However, lack of a similar pattern of hypoautofluorescence as seen in peripapillary cases and presence of just a subtle subretinal grayish hue with intact RPE on SS-OCT/SD-OCT scans in most of the cases of our macular cohort defies the speculated RPE involvement for the macular variants.⁷

The only work giving an insight into the histopathology of the macular variants of combined hamartoma was published by Laqua and Wessing,⁸ who noted RPE hypertrophy or hyperpigmentation without evidence of RPE reduplication or RPE migration anteriorly into the overlying retinal layers. The extenuated pattern of pigmentation (subretinal grayish hue) in macular variants observed in our study could well correspond to the histopathologic description for such lesions.

The presence of full-thickness retinal involvement along with EZ disruption and RPE involvement on OCT of peripapillary combined hamartoma in our analysis (Figure 1) parallels the marked retinal disorganization and replacement of normal architecture of retina and optic nerve by glial vascular tissue on histopathologic description. The greater extent of RPE involvement could be a potential reason for the secondary changes such as choroidal neovascular membranes^{9,10} and vitelliform lesions¹¹ found to be associated with peripapillary combined hamartoma in our cohort as well as in the literature.

OCT findings of maxi peaks, omega sign or sawtooth appearance of OPL, lack of RPE or EZ involvement,⁷ and distorted but still traceable individual retinal layers were consistent with macular combined hamartoma (Figure 2) as described in literature. There was a slender association of these OCT findings with peripapillary combined hamartoma in our analysis owing to the astringent retinal distortion exhibited by this variant.

Our comparative analysis of peripapillary and macular combined hamartoma highlights differences in the morphologic and imaging traits of both variants (representative Figures 3, 4, and 5). The magnitude of retinal involvement and pigmentation observed in peripapillary lesions as compared to the macular lesions suggests a higher grade of retinal distortion or hamartomatous malformation in peripapillary combined hamartoma in comparison to macular combined hamartoma.

In conclusion, using color fundus photography, OCT, and FAF, we found that there is variation in the severity of retinal distortion in peripapillary vs macular combined hamartoma. The peripapillary variants demonstrated greater extent of pigmentation along with retinal and RPE involvement. These clinical and imaging features could potentially lead to a better understanding of the natural progression of each combined hamartoma variant, based on the location of the lesion.

FUNDING/SUPPORT: NO FUNDING OR GRANT SUPPORT. FINANCIAL DISCLOSURES: ADRIAN T. FUNG IS A CONSULTANT TO Allergan Inc. and Bayer. J. Fernando Arevalo is a consultant to Turing Pharmaceuticals LLC, DORC International B.V., Allergan Inc, Bayer, and Mallinckrodt and receives research support from Topcon Medical Systems. K. Bailey Freund is a consultant to Optos, Optovue, Zeiss, Allergan, Novartis, and Heidelberg Engineering and receives research support from Genentech/Roche. The following authors have no financial disclosures: Rajan Gupta, Marco Lupidi, Rajeev R. Pappuru, Sameera Nayak, Niroj Kumar Sahoo, Swathi Kaliki, Lawrence Yannuzzi, Kate Reid, Lianne Lim, Riccardo Sacconi, Vivek Dave, Sumit Randhir Singh, Apoorva Ayachit, Pierre-Henry Gabrielle, Sophie Cai, Luiz H. Lima, Giuseppe Querques, Carol L. Shields, and Jay Chhablani. All authors attest that they meet the current ICMJE criteria for authorship.

REFERENCES

1. Gass J. An unusual hamartoma of the pigment epithelium and retina simulating choroidal melanoma and retinoblastoma. *Trans Am Ophthalmol Soc* 1973;71:171.
2. Vogel MH, Zimmerman LE, Gass JDM. Proliferation of the juxtapapillary retinal pigment epithelium simulating malignant melanoma. *Doc Ophthalmol* 1969;26(1):461–481.
3. Shields CL, Mashayekhi A, Dai VV, Materin MA, Shields JA. Optical coherence tomographic findings of combined hamartoma of the retina and retinal pigment epithelium in 11 patients. *Arch Ophthalmol* 2005;123(12):1746–1750.
4. Arepalli S, Pellegrini M, Ferenczy SR, Shields CL. Combined hamartoma of the retina and retinal pigment epithelium: findings on enhanced depth imaging optical coherence tomography in eight eyes. *Retina* 2014;34(11):2202–2207.
5. Schachat AP, Shields JA, Fine SL, et al. Combined hamartomas of the retina and retinal pigment epithelium. *Ophthalmology* 1984;91(12):1609–1615.
6. Kumar V, Chawla R, Tripathy K. Omega sign: a distinct optical coherence tomography finding in macular combined hamartoma of retina and retinal pigment epithelium. *Ophthalmic Surg Lasers Imaging Retina* 2017;48(2):122–125.
7. Chawla R, Kumar V, Tripathy K, et al. Combined hamartoma of the retina and retinal pigment epithelium: an optical coherence tomography–based reappraisal. *Am J Ophthalmol* 2017;181:88–96.
8. Laqua H, Wessing A. Congenital retino-pigment epithelial malformation, previously described as hamartoma. *Am J Ophthalmol* 1979;87(1):37–42.
9. Theodossiadis PG, Panagiotidis DN, Baltatzis SG, Georgopoulos GT, Moschos MN. Combined hamartoma of the sensory retina and retinal pigment epithelium involving the optic disk associated with choroidal neovascularization. *Retina* 2001;21(3):267–270.
10. Inoue M, Noda K, Ishida S, et al. Successful treatment of subfoveal choroidal neovascularization associated with combined hamartoma of the retina and retinal pigment epithelium. *Am J Ophthalmol* 2004;138(1):155–156.
11. Chae B, Dhrami-Gavazi E, Dansingani KK, Freund KB, Lee W, Yannuzzi LA. Multimodal imaging of combined hamartoma of the retina and retinal pigment epithelium associated with an acquired vitelliform lesion. *Int J Retina Vitreous* 2015;1(1):23.